A Cyto-silicon Hybrid System Interfacing a CMOS Electrode Array with Heart and Brain Cells with On-chip Closed-loop Modulation

*Jun Wang
SEAS, Harvard University
Cambridge, USA
junwang@g.harvard.edu

*Seok Joo Kim
SEAS, Harvard University
Cambridge, USA
sjkim11@seas.harvard.edu

*Wenxuan Wu
SEAS, Harvard University
Cambridge, USA
wenxuanwu@g.harvard.edu

Jongha Lee
SEAS, Harvard University
Cambridge, USA
jonghalee@seas.harvard.edu

Henry Hinton
SEAS, Harvard University
Cambridge, USA
hinton@g.harvard.edu

Rona S. Gertner
CCB, Harvard University
Cambridge, USA
gertner@chemistry.harvard.edu

Han Sae Jung
SEAS, Harvard University
Cambridge, USA
hansaejung@g.harvard.edu

Hongkun Park
CCB, Physics, Harvard University
Cambridge, USA
hongkun_park@harvard.edu

Donhee Ham
SEAS, Harvard University
Cambridge, USA
donhee@seas.harvard.edu

Abstract— We report a mixed-signal CMOS chip with an array of surface electrodes, which is capable of not only electrophysiological recording and stimulation of biological cells but also low-latency closed-loop modulation between the recorded and stimulated cells. To demonstrate the utility of the on-chip closed-loop modulation as an artificial feedback pathway between biological cells, we have developed a silicon-cardiomyocyte self-sustained oscillator with a tunable locked frequency and a silicon-neuron interface that offers an artificial (silicon) inhibitory connection between neurons. These chip-cell interfaces smear the boundary between biological and semiconductor systems.

Keywords—CMOS electrode array, electrophysiology, neurons, cardiomyocytes, bioelectronics.

I. INTRODUCTION

One of the hot pursuits in the electrical interface between biological electrogenic systems—such as heart and brain—and semiconductor chips is to artificially substitute or augment biological functions for applications in prosthesis and brain-machine interface as well as for fundamental biological investigations. Recording electrical signals from a biological system and providing an artificial stimulation back to the biological system based on the recorded signals would be a function essential for such interface. Such closed-loop modulation was pioneered by earlier works [1]-[5], but it was implemented off chip or had long latency. In addition to capability of intracellular recording and stimulation [6], monolithic integration of closed-loop modulation on the same chip is a critical next step to decrease latency in the artificial feedback pathway.

Here, we report a cyto-silicon hybrid system, where a CMOS electrode array coupled to rat cardiomyocytes and neurons performs not only recording and stimulation but also on-chip closed-loop modulation. Each surface electrode of the CMOS chip is connected to its own analog circuit unit inside the chip, which contains a voltage amplifier, an adaptive spike (action potential) detector, and a current injector for recording and stimulation. The CMOS chip also integrates global digital event processors (EPs) for the close-loop modulation. With this mixed-signal CMOS chip, we have developed a silicon-cardiomyocyte self-sustained oscillator whose locked frequency is tuned by the EPs, and a silicon-neuron interface where the chip offers an artificial

inhibitory connection path between neurons. This cell-silicon hybrid system obscures the boundary between the biological and semiconductor systems.
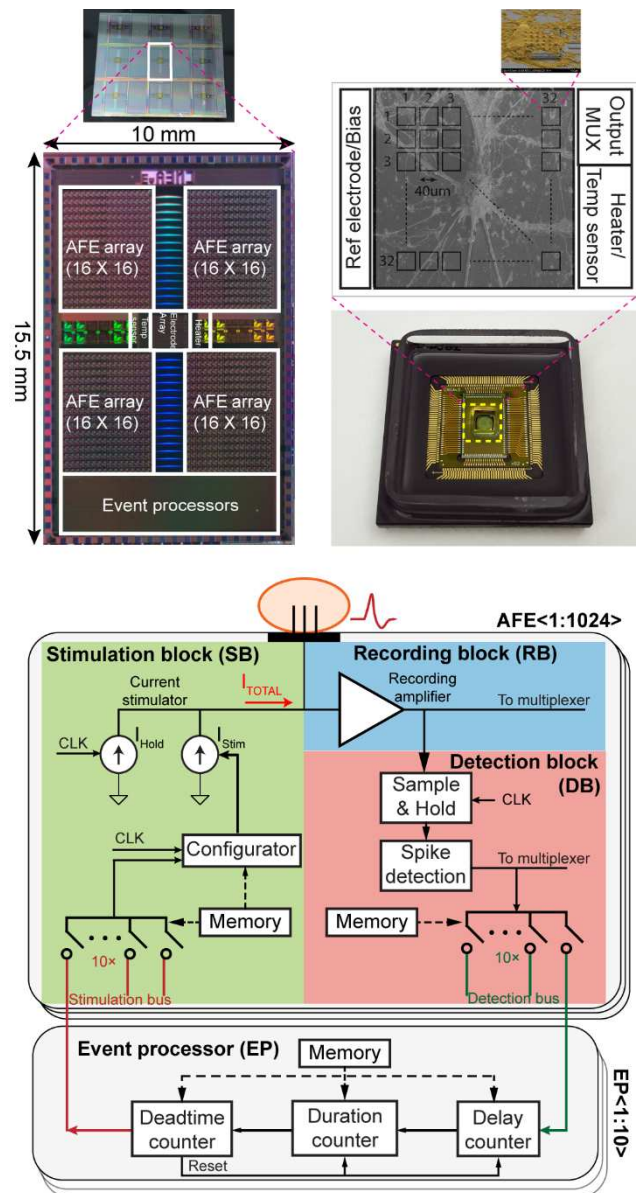

Fig. 1. Photos (top) and architecture (bottom) of the CMOS integrated circuit, which contains 10 global event processors and an array of 1,024 AFE pixels.

II. CMOS CHIP ARCHITECTURE

Fig. 1, top, displays a photograph of the CMOS chip and an examplary packaged chip with an SEM image insert showing neurons sitting on the nanoneedles post-fabricated on top of the CMOS. The post-fabrication and packaging protocols are detailed in the Methods session of reference [6].

Fig. 1, bottom, shows the architecture of the CMOS chip. It comprises an array of $4 \times 16 \times 16 = 1,024$ analog front-end (AFE) circuit units, or 'pixels,' with each pixel connected to its own electrode on the chip surface, and 10 globally shared digital EPs. Each AFE pixel contains recording, detection, and stimulation blocks (RB, DB, and SB). An electrophysiological signal from a biological cell coupled to an electrode of a pixel is amplified by the pixel's RB and then fed to the spike detector in the pixel's DB, which converts each detected action potential (spike) into a digital pulse and transmits to an EP through a shared detection bus. The EP responds by transmitting a configuration signal to a destination pixel through a shared stimulation bus. The SB of this destination pixel then injects a stimulation current to its own electrode, where the timing and duration of the current injection is programmed in the configuration signal from the EP. This completes the closed-loop modulation pathway. While we have just described a loop connecting a single recording pixel and a single destination (stimulation) pixel via a single EP for the sake of simplicity, any single recording or destination pixel can be connected to up to 10 EPs, and each EP can be connected up to all 1,024 pixels. As an aside, we note that both RB and spike detector outputs in the on-chip closed-loop modulation pathway are also multiplexed out to an off-chip measurement system to confirm the workings of the chip.

III. CIRCUIT BLOCKS

Here we describe each key function block of the CMOS chip in details and present characterization results.

A. Recording block (RB)

Fig. 2, top, shows the schematic of the RB, essentially an op-amp with a negative feedback. This RB amplifier can be configured into various recording modes with 7 switches. In our experiment, we employ it primarily as an AC-coupled bandpass amplifier, whose gain and cutoff frequencies are tuned by the adjustable input and feedback capacitors and
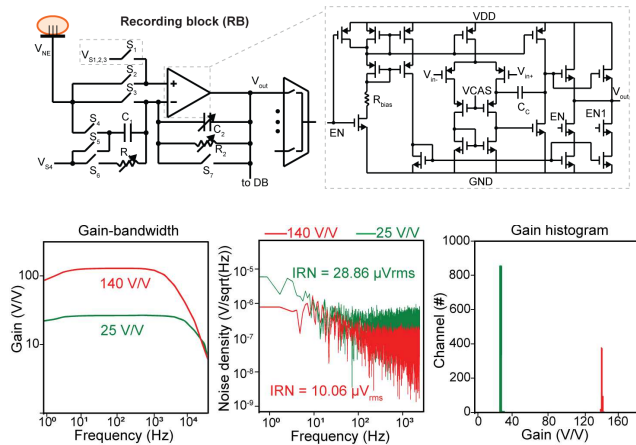

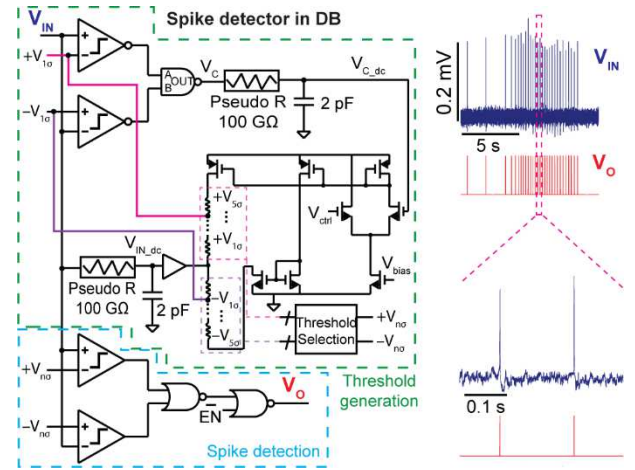Fig. 2. RB amplifier schematic and characterization results.

Fig. 3. Schematic and measurements of an adaptive spike detector.

resistors. Fig. 2, bottom, shows the measured gain and input referred noise of a representative RB amplifier for intracellular and extracellular recording scenarios, as well as the histogram of measured gains for all 1,024 RB amplifiers. To reduce 1/f noise, big transistors are used in the RB design.

B. Detection block (DB)

Fig. 3, left, shows the schematic of the DB, which is a spike detector. The negative feedback loop of the spike detector (dashed green box) contains two comparators, a NAND gate, an *RC* low-pass filter, a differential pair, and a resistive network. This negative feedback loop sets ten threshold voltages $\pm V_{n\sigma}$ ($n = 1, 2, 3, 4,$ and 5), which are at voltages $n\alpha$ above and below the baseline of the input voltage V_{IN} (amplified electrophysiological signal). Here, the negative feedback determines the magnitude of α based on the noise level of the V_{IN} baseline, with α growing with
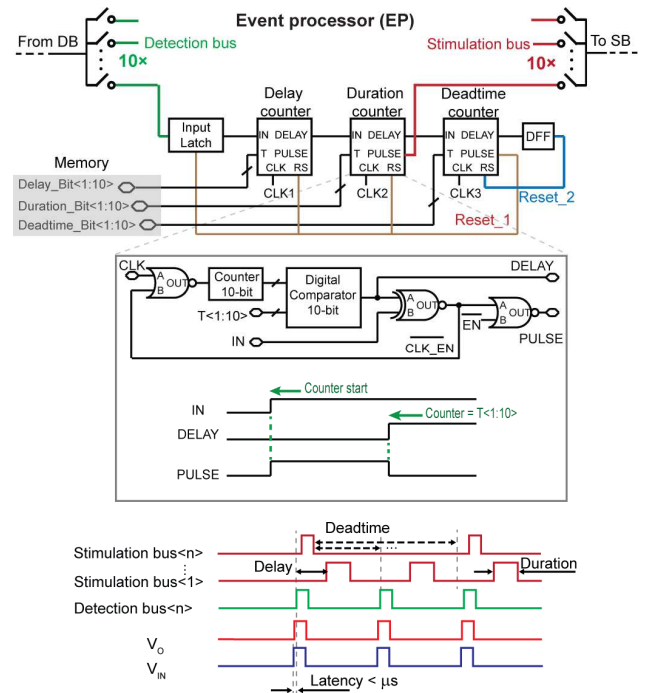

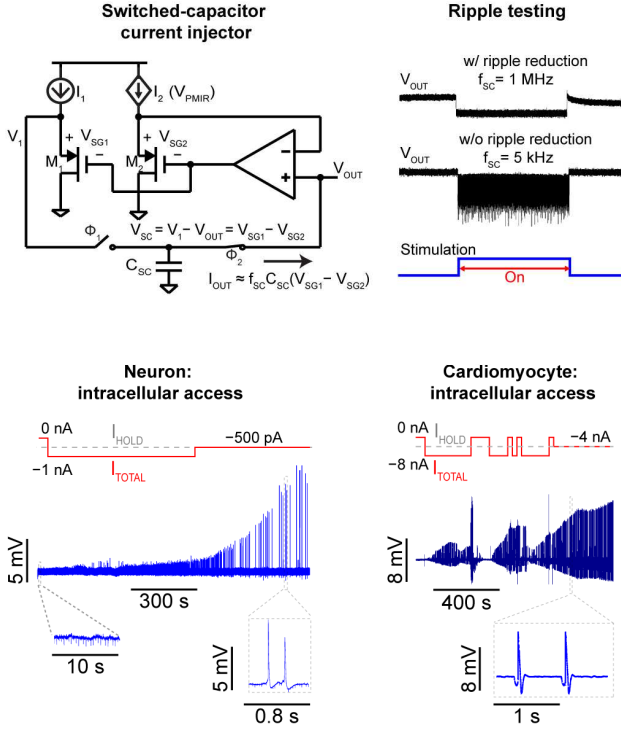Fig. 4. Schematic and operation of an event processor.

Fig. 5. (Top) Switched-capacitor current injector and experimental verification of ripple removal; (bottom) Intracellular coupling and stimulation with neurons and cardiomyocytes based on current injection.

the noise level. In other words, the threshold voltages are set adaptively. In the lower part of the spike detector (dashed blue box), we choose any one of n for $\pm V_{n\sigma}$ and compare V_{IN} to the chosen $\pm V_{n\sigma}$, which leads to a spike detection. A higher n gives a more conservative criterion for spike detection (we typically set n at 3 or 4 for intracellular recording, and 1 or 2 for extracellular recording). Each detected spike is converted to a digital pulse by the combinational logic in the dashed blue box, which serves as the DB output V_O. Fig. 3, right, shows an experimental example of a spike detection with an intracellular neuronal recording ($n = 3$).

C. Event processor (EP)

Fig 4, top, shows a schematic of an EP, which contains delay, duration, and deadtime counters. The three blocks have exactly the same logic circuit (Fig. 4, middle), but the delay and deadtime counters are tapped at the DELAY node for their outputs, while the duration counter is tapped at the PULSE node for its output. The three blocks together program the configuration signal to be transmitted to the SB of a destination pixel: the configuration signal dictates the timing and duration of the current injected by the SB. The EP also contains an input latch to lock to a selected detection bus state upon a spike detection. The latch will not be reset until the configuration signal is delivered to a destination pixel and the deadtime passes. Fig. 4, bottom, shows timing diagrams for the amplified electrophysiological signal V_{IN}, the spike detector output V_O transmitted to an EP through detection bus n ($n = 1, 2, …, 10$), and configuration signals transmitted through stimulation bus n ($n = 1, 2, …, 10$). Since there is no off-chip processing, the intrinsic latency is less than 1 ms, enabling our chip to provide closed-loop stimulation with a ms resolution. The resolution is determined by the clock frequency of counters that can run beyond MHz.
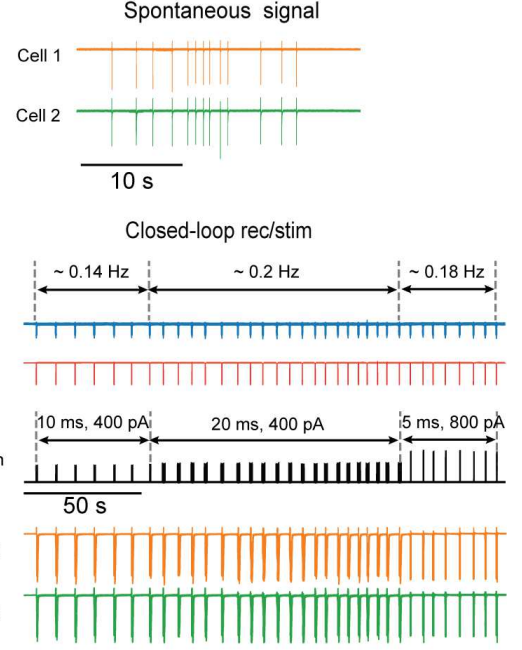

Fig. 6. Closed-loop modulation experiments with cardiomyocytes.

D. Stimulation block (SB)

The two current injectors (I_{STIM} & I_{HOLD}) in the SB (Fig. 1) have the identical switched-capacitor circuit topology of Fig. 5, offering high output impedance [7]. In this topology, the injected current is $f_{SC} \times C_{SC} \times (V_{SG1}-V_{SG2})$ where f_{SC} is the switching frequency, C_{SC} is the switched capacitor, and V_{SG1} and V_{SG2} are the source-gate voltages of the two pFETs. We adjust the biases of the two FETs in such a way to make $|V_{SG1}-V_{SG2}|$ small enough, so that the typical injection current can be obtained with an f_{SC} that is far beyond
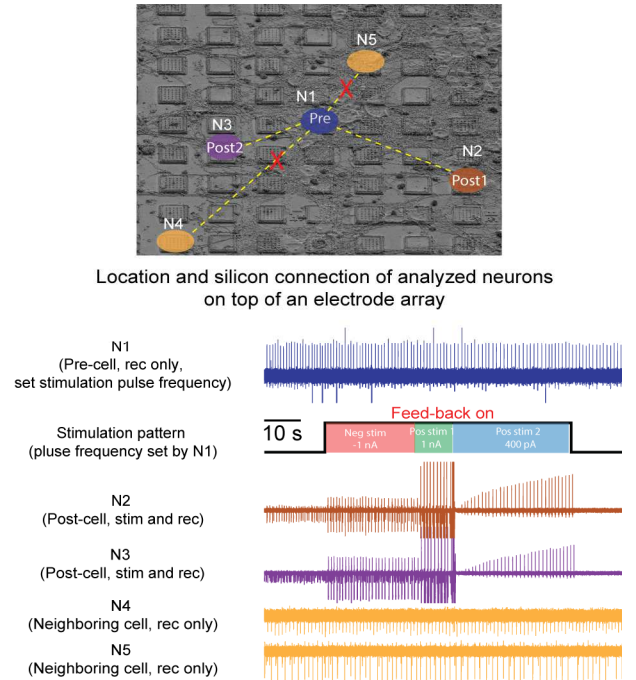

Fig. 7. Closed-loop modulation experiments with neurons.

the electrophysiological signal band. This is to ensure that

the ripple voltage [7] unavoidable with the switched capacitor circuit is filtered out by the RB amplifier, whose bandwidth is on par with the electrophysiological signal band, so that the switched-capacitor current injector does not interfere with the electrophysiological recording at RBs (Fig. 5, top). Back to Fig. 1, the current injector I_{HOLD} injects a constant current, while the current injector I_{STIM} injects a modulated current, whose timing and duration are controlled by the configuration signal from an EP, and polarity and amplitude by the sign of V_{SG1}-V_{SG2} and the switching frequency f_{SC}, respectively. The resulting current injection, I_{HOLD} + I_{STIM}, with the duration, polarity, and amplitude modulation is used to permeabilize a cell—which can lead up to intracellular coupling—and stimulate it [6]. Fig. 5, bottom, shows example measurements where the current injection is used to obtain intracellular access and stimulation with neurons and cardiomyocytes.

IV. CLOSED-LOOP MODULAITON EXPERIMENTS

A. Experiments with cardiomyocytes

Fig. 6, shows an experiment with a tissue of cardiomyocytes cultured on top of the CMOS chip. The extracellular recording by the CMOS chip shows that the network of cardiomyocytes exhibits a spontaneous synchronized network oscillation before closed-loop modulation (Fig. 6, top); *i.e.*, all cardiomyocytes are locked to the same beating (spiking) rate. We subsequently provide closed-loop pathways from one recording pixel (labeled Pre-cell in Fig. 6) to 16 destination pixels (labeled Post-cells in Fig. 6, showing two of them). The current injections in the 16 destination pixels then occur in a repeated manner, with the repetition frequency locked to the network oscillation frequency. While the frequency is locked, we can modulate the duration and amplitude of each current injection, which leads to the tuning of the network oscillation frequency (the stimulation that leads to this network dynamics modification is possibly due to permeabilization) (Fig. 6). The frequency of the current injection repetition is always locked to the network oscillation frequency, and thus tracks the change. This is a silicon-cardio hybrid oscillator, with the artificial feedback pathway serving to modify the network dynamics.
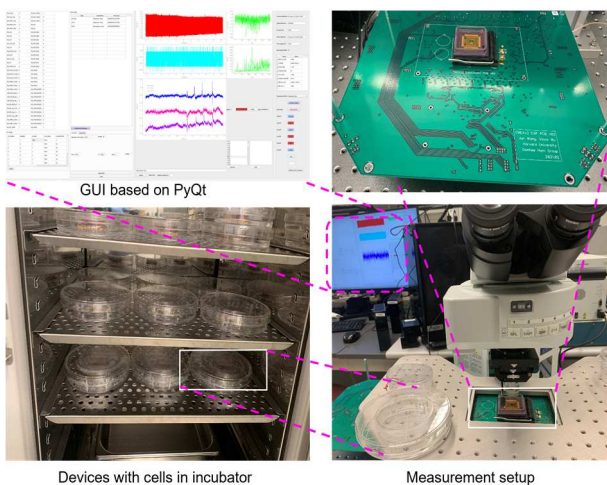

Fig. 8. Experimental setup.

TABLE I. COMPARISON WITH OTHER RELEVANT WORK

		This work	[2]	[3]	[4]	[5]	[7]
Technology (nm)		**180**		180		180 HV	180
Rec/ Stim	No.Ch	**1024/ 1024**	32/	8/8	126/ 42	12	4096/ 4096
	Intracellular	**Yes**	No	No	No	No	Yes
Stimulation type		**V & I**		I	V	I	V & I
Closed-loop	On/Off-chip	**On-chip**	Soft ware	Multi ICs	Off-chip	On-chip	N/A
Minimum latency		**Sub μs**	Tens ms	Sub ms	Sub ms	Sub ms	N/A

B. Experiments with neurons

Fig. 7, shows an experiment with rat cortical neurons cultured on the CMOS chip (in this particular case the neurons are not as densely connected as in the cardiomyocyte tissue). The neurons exhibit spontaneous activities, as confirmed by the CMOS chip's intracellular recording. We then provide closed-loop pathways from one pixel that is performing an intracellular recording (N1) to two destination pixels (N2 and N3). These artificial pathways through the CMOS chip's EPs do not affect the spontaneous activities in N2 and N3 when current injections in response to N1 activities are negative, but positive current injections in response to N1 activities suppress the spontaneous activities of N2 and N3. This is an artificial inhibitory pathway between neurons (N1 and N2; and N1 and N3) provided via the CMOS chip. Two pixels, N4 and N5, to which we do not provide closed-loop signal pathways, are not affected at all. Figure 8 shows the measurement setup, and Table I presents a comparison with other relevant work.

V. CONCLUSION AND DISCUSSION

We have reported a mixed-signal CMOS integrated circuit consisting of an array of 1,024 analog circuit units and 10 event processors, which together provide the capability for electrophysiological recording and stimulation, and importantly, the capability for low-latency closed-loop modulation between recorded and stimulated cells. Using this chip, we have demonstrated a silicon-cardiomyocyte self-sustained oscillator with a tunable locked frequency, and a silicon-neuron interface that provides artificial (silicon) inhibitory connection pathways between neurons. Compared to an open-loop pacemaker, a closed loop silicon-cardiomyocyte self-sustained oscillator has the ability to adjust its beating frequency to adapt to the changes in physiological conditions. A silicon inhibitory connection pathway between neurons has the potential to benefit epilepsy patients. However, it would be even more exciting to explore further to achieve both inhibitory and excitatory pathways between artificial and biological neurons.

These experiments represent a path forward for dynamically tuning a system that hybridizes biological electrogenic cells and neuromorphic components with integrated artificial signal pathways connecting the biological cells, ultimately enhancing nervous system [8], [9]. To make the presented system suitable for *in-vivo* applications, integration of a probe extending the sensing/stimulation electrodes is necessary [10]. To further make the whole system implantable, techniques like digital CDS [11] to reduce 1/f noise while keeping the analog front end small, and features like wireless powering and data transmission [12], [13], will be helpful.

REFERENCES

[1] A. A. Prinz, L. F. Abbott, and E. Marder, "The dynamic clamp comes of age," Trends Neurosci., vol. 27, no. 4, pp. 218–224, 2004, doi: https://doi.org/10.1016/j.tins.2004.02.004.

[2] Q. Zhang et al., "A prototype closed-loop brain–machine interface for the study and treatment of pain," Nat. Biomed. Eng., 2021.

[3] Y. Wang, Q. Sun, H. Luo, X. Chen, X. Wang, and H. Zhang, "26.3 A Closed-Loop Neuromodulation Chipset with 2-Level Classification Achieving 1.5Vpp CM Interference Tolerance, 35dB Stimulation Artifact Rejection in 0.5ms and 97.8% Sensitivity Seizure Detection," ISSCC, 2020.

[4] J. Müller, D. Bakkum, and A. Hierlemann, "Sub-millisecond closed-loop feedback stimulation between arbitrary sets of individual neurons," Front. Neural Circuits, vol. 6, no. DEC, pp. 1–11, 2012.

[5] X. Liu et al., "A 12-channel bidirectional neural interface chip with integrated channel-level feature extraction and PID controller for closed-loop operation," in 2015 IEEE Biomedical Circuits and Systems Conference (BioCAS), 2015, pp. 1–4, doi: 10.1109/BioCAS.2015.7348339.

[6] J. Abbott et al., "A nanoelectrode array for obtaining intracellular recordings from thousands of connected neurons," Nat. Biomed. Eng., vol. 4, no. 2, pp. 232–241, 2020.

[7] J. Abbott *et al.*, "The design of a CMOS nanoelectrode array with 4096 current-clamp/voltage-clamp amplifiers for intracellular recording/stimulation of mammalian neurons," *IEEE J. Solid-State Circuits*, vol. 55, no. 9, pp. 2567–2582, 2020, doi: 10.1109/JSSC.2020.3005816.

[8] Frédéric D Broccard et al., "Neuromorphic neural interfaces: From neurophysiological inspiration to biohybrid coupling with nervous systems," J. Neural Eng., vol. 14, no. 4, p. 041002, 2017, doi: 10.1088/1741-2552/aa67a9.

[9] E. Donati and G. Indiveri, "Neuromorphic bioelectronic medicine for nervous system interfaces: from neural computational primitives to medical applications," Prog. Biomed. Eng., vol. 5, no. 1, p. 13002, Feb. 2023, doi: 10.1088/2516-1091/acb51c.

[10] N. A. Steinmetz et al., "Neuropixels 2.0: A miniaturized high-density probe for stable, long-term brain recordings," Science (80-.)., vol. 372, no. 6539, 2021, doi: 10.1126/science.abf4588.

[11] A. Paul et al., "Neural Recording Analog Front-End Noise Reduction with Digital Correlated Double Sampling," in 2022 IEEE Biomedical Circuits and Systems Conference (BioCAS), 2022, pp. 149–152, doi: 10.1109/BioCAS54905.2022.9948618.

[12] R. Muller, M. M. Ghanbari, and A. Zhou, "Miniaturized Wireless Neural Interfaces: A tutorial," IEEE Solid-State Circuits Mag., vol. 13, no. 4, pp. 88–97, 2021, doi: 10.1109/MSSC.2021.3111387.

[13] A. Akinin et al., "18.1 An Optically-Addressed Nanowire-Based Retinal Prosthesis with 73% RF-to-Stimulation Power Efficiency and 20nC-to-3μC Wireless Charge Telemetering," in 2021 IEEE International Solid- State Circuits Conference (ISSCC), 2021, vol. 64, pp. 276–278, doi: 10.1109/ISSCC42613.2021.9365750.